Electronic Supplementary Material (ESI) for Physical Chemistry Chemical Physics.

Molecular Insights on the Dynamic Stability of Peptide Nucleic Acid Functionalized Carbon and Boron Nitride Nanotubes

Nabanita Saikia,[*#] Mohamed Taha,[⊥] and Ravindra Pandey[*#]

[#]Department of Physics, Michigan Technological University, 1400 Townsend Drive, Houghton, Michigan 49931, United States

[⊥]Materials Science and Nanotechnology Department, Faculty of Postgraduate Studies for Advanced Sciences (PSAS), Beni-Suef University, Egypt.

Table S1. Partial charges of PNA atoms. The atom no. corresponds to the numbering scheme shown in Figure S1.

Atom No.	Atom Type	Partial charge (e)
O_{107}	O	-0.51
C_{106}	C	0.51
C_{105}	CT2	-0.18
H_{123}, H_{122}	HB	0.09
N_{108}	NH1	-0.46
C_{103}	C	0.51
O_{104}	O	-0.51
C_{102}	CT2	-0.01
H_{121}, H_{120}	HB	0.09
C_{109}	CT2	-0.18
H_{125}, H_{124}	HA	0.09
C_{110}	CT2	-0.18
H_{127}, H_{126}	HA	0.09
N_{111}	NH1	-0.46
H_{128}	H	0.31

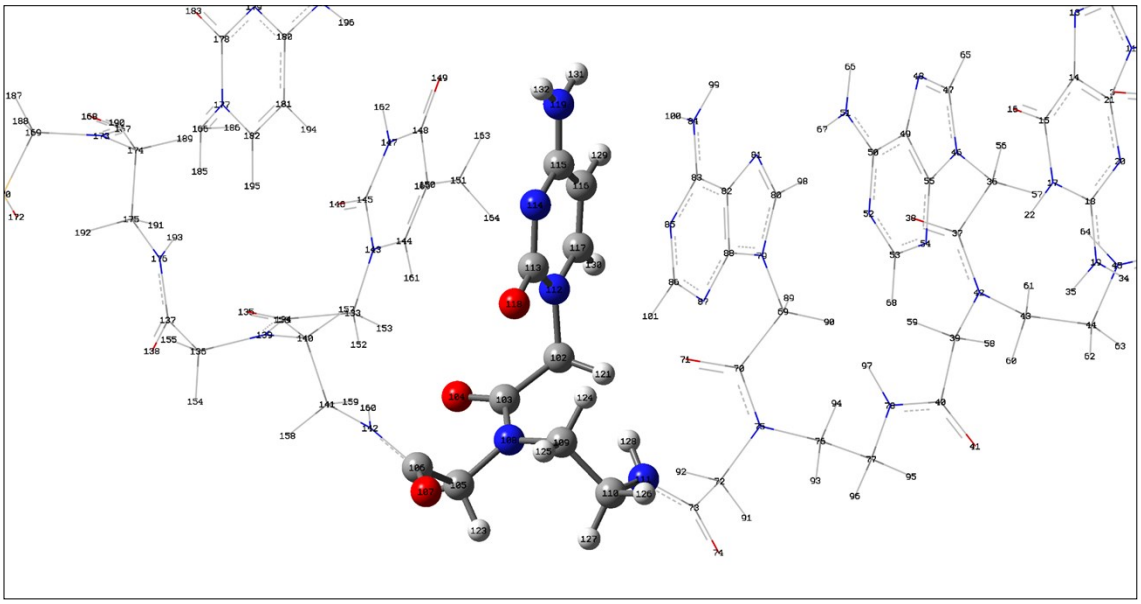

Figure S1. The 6-mer PNA oligopeptide considered for MD simulation. The partial charges of the reference atoms in ball and stick are shown in Table S1.

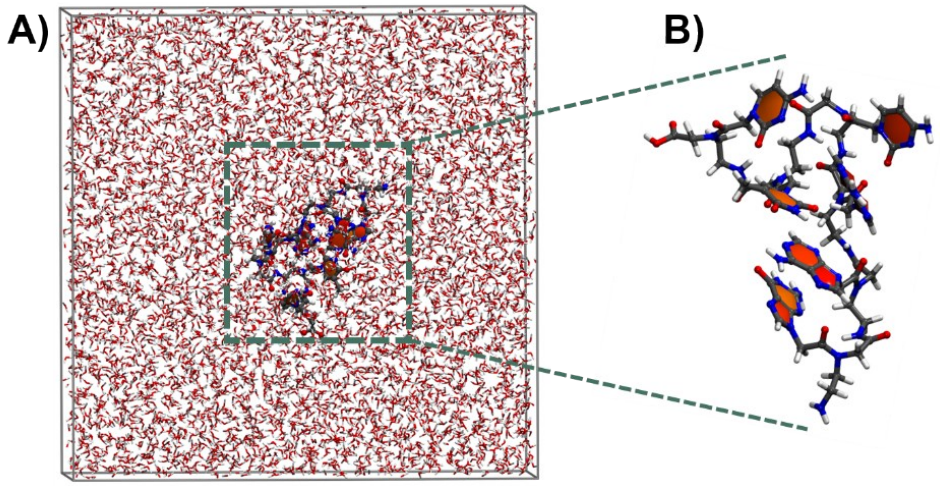

Figure S2. Simulation snapshot at 50 ns of a 6-mer PNA oligopeptide in aqueous solution.

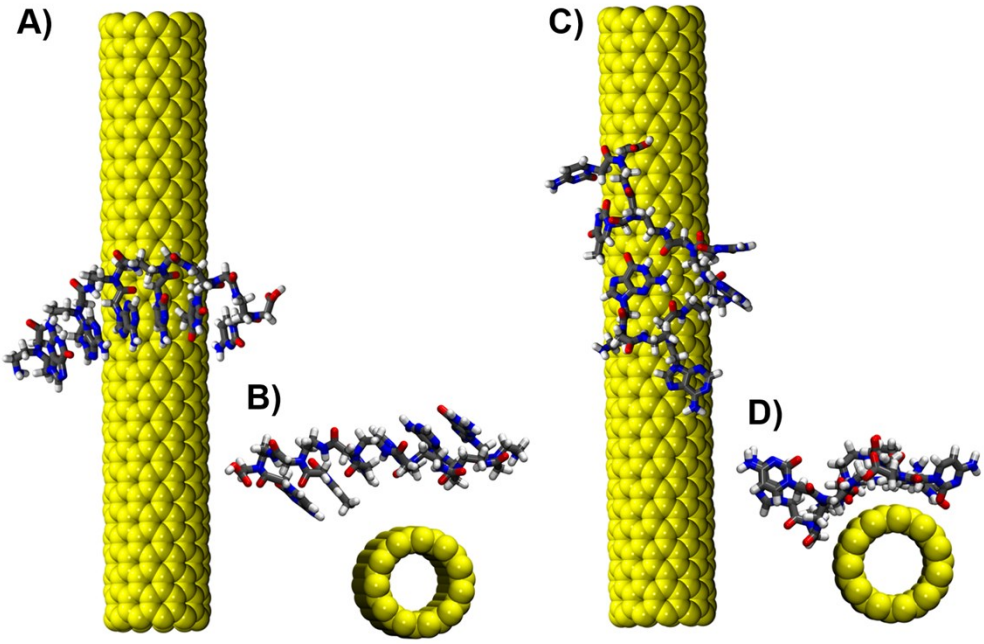

Figure S3. (A) Side and (B) front views of initial configuration of PNA rotated at ~ 90^0 with respect to tubular axis of CNT. (C-D) 50 ns snapshot of CNT/PNA hybrid depicting the orientation and assembly of PNA.

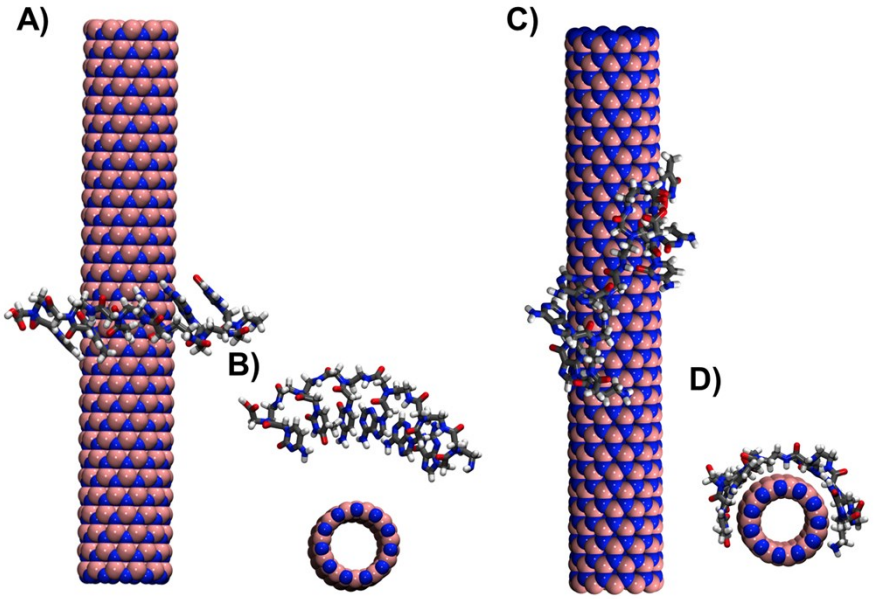

Figure S4. (A) Side and (B) front views of initial configuration of PNA rotated at ~ 90^0 with respect to tubular axis of BNNT. (C-D) 50 ns snapshot of BNNT/PNA hybrid depicting the orientation of PNA.

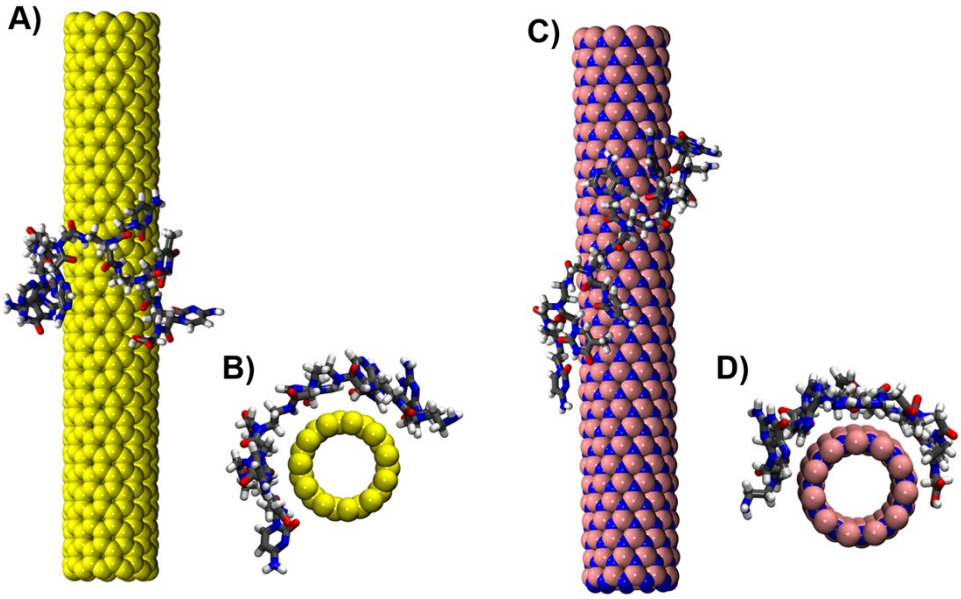

Figure S5. Simulation snapshot at 50 ns for (A-B) CNT/PNA and (C-D) BNNT/PNA hybrids. PNA was aligned along the nanotube at an initial distance of ~20.0 Å.

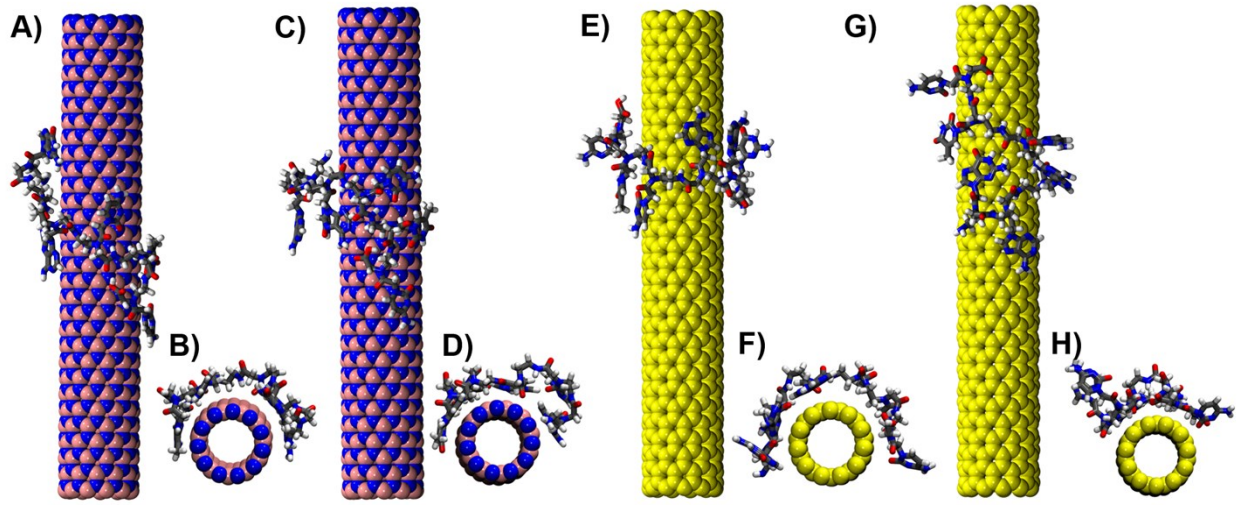

Figure S6. Simulation snapshots from two single trajectory runs with different initial configurations of PNA along the tubular surface. (A-D) BNNT/PNA hybrid and (E-H) CNT/PNA hybrid in aqueous solution. The water molecules are not shown for clarity.

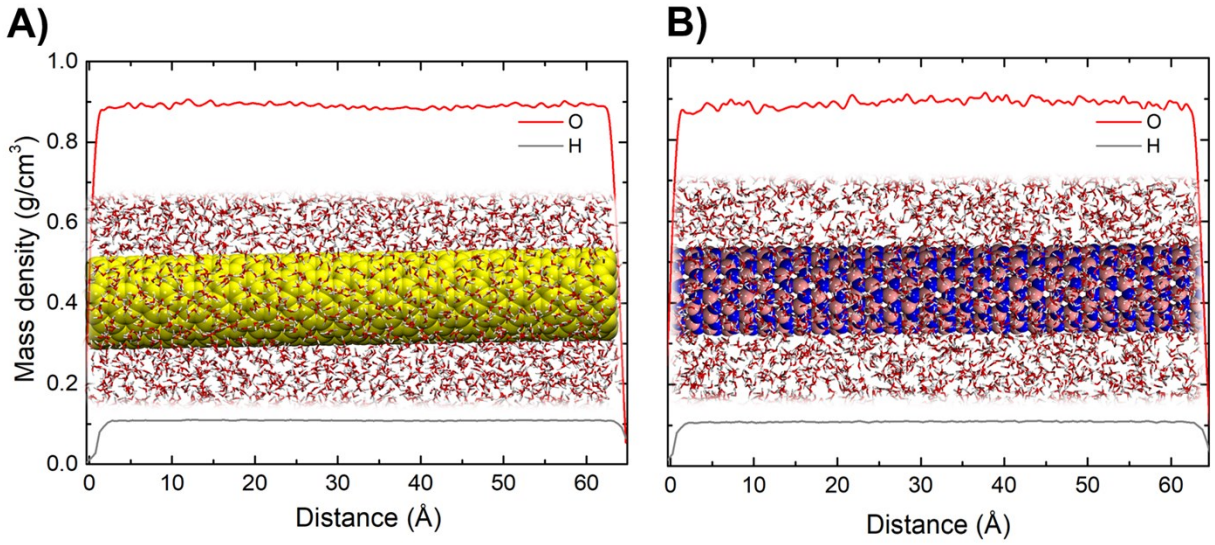

Figure S7. Mass density profile of water in (A) CNT/PNA and (B) BNNT/PNA hybrids.

***Contact area*:** The contact area between CNT (BNNT) and PNA is given by:

$$\text{Contact area} = \tfrac{1}{2}\,[\{SAS_{CNT} + SAS_{PNA}\} - SAS_{CNT/PNA}] \quad (3)$$

where SAS (i.e. solvent accessible surface) is defined as the surface area of a system that is accessible to the solvent We have taken SAS to be representative of the extent of binding-induced conformational changes in PNA. An increase in the SAS value reflects an extension of PNA interacting with CNT (BNNT) relative to the free-standing case.

The predicted contrast in wrapping of PNA on CNT and BNNT is further confirmed by the calculated contact area which is calculated to be 4.9 and 5.1 nm^2 in CNT/PNA and BNNT/PNA hybrids, respectively. Note that SAS for CNT (BNNT) is 3925 (4165) nm^2. PNA has SAS values of 1912.72 and 1961.28 nm^2 in CNT/PNA and BNNT/PNA hybrids, respectively (Figure S8). The semi-ionic nature of B–N bond may be suggested to maximize the base-surface interactions. A previous study reported a contact area of ~6.3 nm^2 for polyalanine/(12,12) BNNT hybrid.[1] Note that SAS for CNT and BNNT in absence of PNA was calculated as 3925 (4165) nm^2. PNA has SAS values of 1912.72 and 1961.28 nm^2 in CNT/PNA and BNNT/PNA hybrids, which suggests that the semi-ionic nature of B–N bond may assist in maximizing the base-surface interactions.

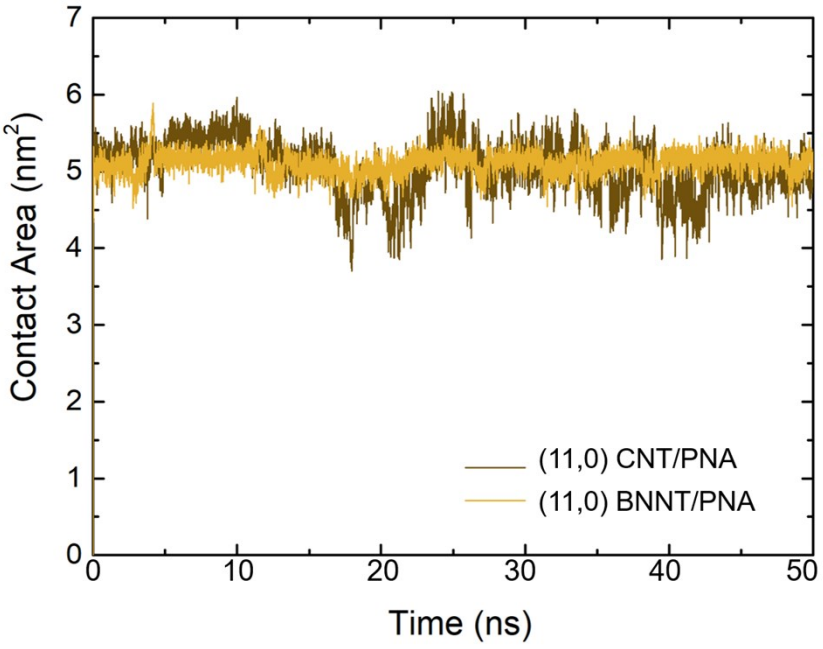

Figure S8. Calculated contact area for CNT/PNA and BNNT/PNA hybrids.

The root mean square fluctuations (RMSF) analysis can help to predict which of the PNA regions interact with the tubular surface over the course of MD simulation. RMSF of PNA in close proximity to nanotube tubular surface is shown in Figure S9. Although PNA is quite flexible, RMSF of cytosine, thymine and adenine nucleobases are higher in comparison to the polypeptide backbone, and interaction of PNA along the nanotube sidewall is mainly intermediated by the nucleobases.

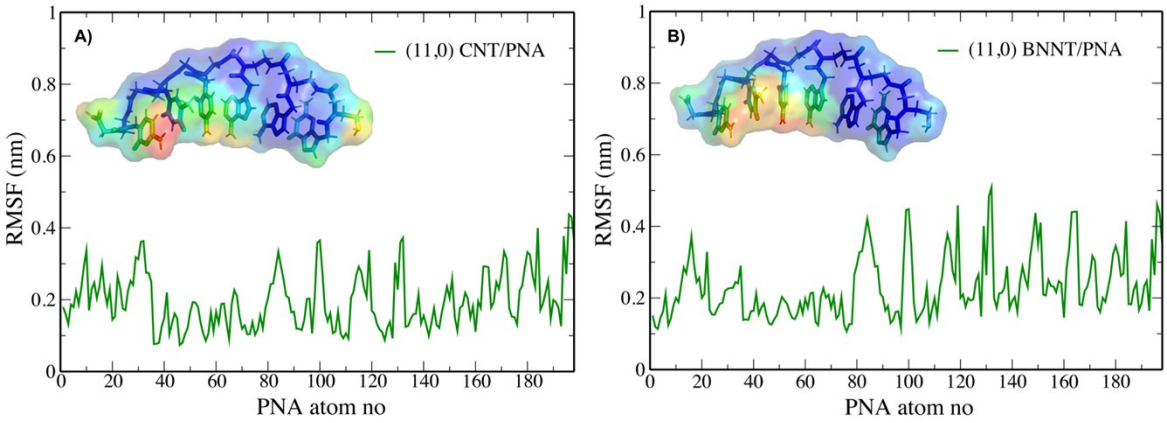

Figure S9. RMSF plots of PNA in (A) (11,0) CNT/PNA and (B) (11,0) BNNT/PNA. The inset figures illustrate the RMSF mapped on PNA atoms. The red regions represent the atoms that exhibit pronounced flexibility and blue regions have lower fluctuations and are less dynamic.

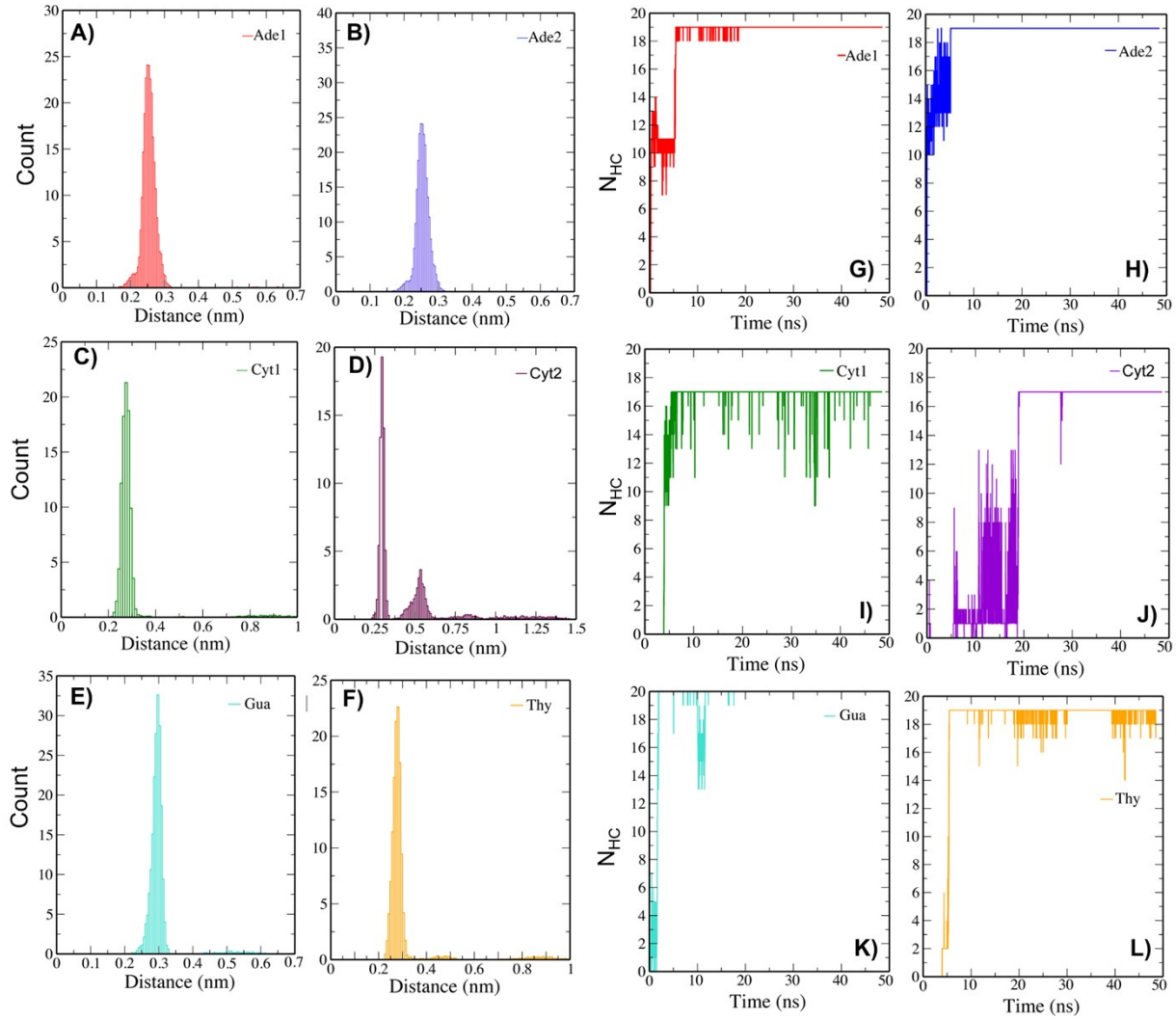

Figure S10. (A-F) Histograms of the minimum interacting distance between the individual PNA nucleobases and BNNT sidewall. (G-L) Number of hydrophobic contacts between the nucleobases and BNNT sidewall.

Figure S11 confirms the fact that a higher degree of iconicity at the tubular surface significantly modifies the interface yielding distinctly different assembly of PNA polypeptide backbone and stacking of nucleobases along the tubular surface of BNNT. Simulations performed with partial charge of ± 0.975e on B (N) atoms resulted in the absence of the base stacking on the tubular surface. The nucleobases aligned away from nanotube tubular surface of BNNT (Figure S11A and B).

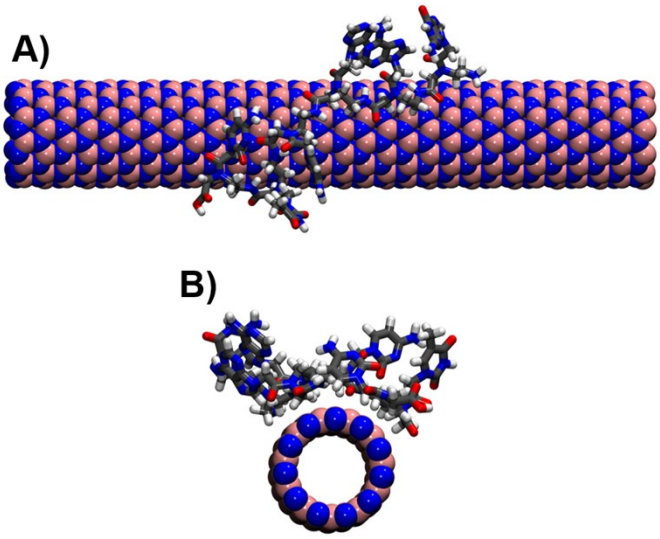

Figure S11. 50 ns snapshots of BNNT/PNA hybrid with partial charge of ± 0.975e on B (N) atoms. (A) side view and (B) front view. The water molecules are not shown for clarity.

Reference

(1) Mudedla, S. K.; Balamurugan, K.; Subramanian, V. Unravelling the Structural Changes in α-Helical Peptides on Interaction with Convex, Concave, and Planar Surfaces of Boron- Nitride-Based Nanomaterials. *J. Phys. Chem. C* **2016**, *120*, 28246−28260.